Acta Oceanol. Sin., 2023, Vol. 42, No. 4, P. 33–40
https://doi.org/10.1007/s13131-022-2088-z
http://www.aosocean.com
E-mail: ocean2@hyxb.org.cn

Sedimentary nitrogen dynamics in a coastal reef area with relatively high nitrogen concentration

Zhiming Ning[1], Ronglin Xia[1], Bin Yang[2]*, Cao Fang[1], Wei Jiang[1], Guodong Song[3]

[1] Guangxi Laboratory on the Study of Coral Reefs in the South China Sea, School of Marine Sciences, Guangxi University, Nanning 530004, China

[2] Guangxi Key Laboratory of Marine Environmental Change and Disaster in Beibu Gulf, Beibu Gulf University, Qinzhou 535011, China

[3] Key Laboratory of Marine Chemistry Theory and Technology of Ministry of Education, Ocean University of China, Qingdao 266100, China

Received 7 February 2022; accepted 24 June 2022

Abstract

The migration and transformation of nitrogen (N) in sediments play an important role in regulating the N concentration and nutrient structures in shallow seas. However, studies of sedimentary N dynamics are rarely focused on carbonate sediments, although these account for about 40% of the continental shelf area. Thus, the regulation mechanisms of the N dynamics in the carbonate sands of coral reefs are not clear. Taking the coral reef area of Weizhou Island, which has a relatively high N concentration, as the research object, we conducted a series of flow-through reactor experiments to investigate the fluxes of different N forms at the interface of sediment and seawater and their regulation mechanism by environmental factors. The fluxes of dissolved inorganic and organic N (DIN and DON) at different stations were –0.39–0.12 mmol/(m^2·h) and –0.18–0.39 mmol/(m^2·h), respectively. Denitrification (0.11–0.25 mmol/(m^2·h)) was closely coupled to nitrification, which was limited by the availability of organic matter and its degradation product (i.e., NH_4^+). Thus, the excessive NO_3^- might be reduced to NH_4^+ by dissimilatory nitrate reduction to ammonium, rather than to N_2 by denitrification. NO_3^- reduction peaked at intermediate advection rates (96 L/(m^2·h)) and flow path lengths (10 cm), but the release of DON also peaked at the same condition. In addition, climate warming would significantly affect sedimentary N dynamics at Weizhou Island. These results may help address the broader issue of the N cycle in coral reef ecosystems under the dual pressure of climate warming and anthropogenic activities, and these results are beneficial to coral reef protection and local ecological management.

Key words: nitrogen dynamics, sediments, coral reefs, Weizhou Island

Citation: Ning Zhiming, Xia Ronglin, Yang Bin, Fang Cao, Jiang Wei, Song Guodong. 2023. Sedimentary nitrogen dynamics in a coastal reef area with relatively high nitrogen concentration. Acta Oceanologica Sinica, 42(4): 33–40, doi: 10.1007/s13131-022-2088-z

1 Introduction

Coral reefs have the most abundant marine biological resources, and thus, the serious degradation of coral reefs around the world has attracted extensive attention (Eakin et al., 2019; Hughes et al., 2003). Although coral thermal bleaching caused by climate warming is considered to be the main factor of coral reef degradation worldwide (Hughes et al., 2017), coral bleaching caused by excess nitrogen (N) generated and discharged by anthropogenic activities in coral reefs at relatively high latitudes should not be ignored (Morris et al., 2019; Wiedenmann et al., 2013; Rosset et al., 2017).

Due to the influence of anthropogenic activities, the nutrient structure in coastal waters of China often has an excess of N (Guo et al., 2019; Ning et al., 2020; Xie et al., 2021), whereas the nutrient exchanges between the seawater and sediment interface play an important role in regulating the N concentration and nutrient structure in shallow reefs (Ning et al., 2019; Rasheed et al., 2003; Eyre et al., 2008). Carbonate sands are the dominant sediments in reef environments, and their porous structure leads to greater porosity and permeability and a microbial abundance of carbonate sand compared to silicate sand (Wild et al., 2005; Rasheed et al., 2003). Thus, the N dynamics of these two sedimentary types are supposed to be different (Kessler et al., 2014; Cook et al., 2017). However, studies on N dynamics in carbonate sands are very rare, and the regulation mechanisms of the sedimentary N dynamics in coral reefs are unclear (Erler et al., 2014; Robertson et al., 2019).

Weizhou Island reef is located in a relatively high latitude area in the northern South China Sea (Fig. 1) and is often threatened by eutrophication attributed to anthropogenic activities (Yu et al., 2019). Anthropogenic activities have altered the global N cycle (Yang and Gruber, 2016; Wang et al., 2019), but their perturbation of N dynamics in reef sediments is not clear, so the N cycle in coral reefs could not be clearly understood. In this study, rising temperatures indicate climate warming, and enrichments of NO_3^- in seawater and total organic carbon (TOC) in sediments are the alternative indicators of anthropogenic activities. We hypothesize that the sedimentary N flux in coral reefs would

Foundation item: The Guangxi Natural Science Foundation under contract Nos 2019GXNSFAA185001 and 2019GXNSFAA185022; the National Natural Science Foundation of China under contract Nos 41976059 and 42166002.
*Corresponding author, E-mail: binyang@bbgu.edu.cn

be stimulated by climate warming and anthropogenic activities. In order to test this hypothesis, we conducted repacked flow-through reactor experiments to investigate the fluxes of different N forms at the interface of sediment and seawater at Weizhou Island, and analyzed their regulation mechanism by environmental factors, including temperature, NO_3^- concentration, the content of TOC in sediments, porewater advection rates, and flow path lengths. With these comprehensive data, we were able to unveil the N dynamics in reef sediments under the influences of climate warming and anthropogenic activities.

2 Materials and methods

2.1 *Study site and sampling*

Weizhou Island is a volcanic island located in the Beibu Gulf, and its relatively high latitude provides an ideal habitat for coral growth. Carbonate sands are the dominant sediments in reef environments, and coupled with the input of terrigenous weathering products, admixed terrigenous silicate and reef-derived carbonate components can be found in the tidal flats of Weizhou Island. During September 2019 at stations in the tidal flats (Fig. 1), seawater samples were collected by submersing a 10 L polyethylene bucket, and sediments (0–10 cm) were collected by pushing Plexiglas tubes (inner diameter of 10 cm) into the sediment. At the same time, 100 mL of surface seawater samples for nutrient analysis were filtered with 0.45 μm pore-size syringe polyethersulfone filters, and Rhizon soil moisture samplers (19.21.23F Rhizon CSS) were pushed into the sediment in the field to collect and filter porewater samples. The blanks of NH_4^+, NO_2^-, and NO_3^- were 0.10 μmol/L, <0.01 μmol/L, and 0.01 μmol/L for syringe filters and 0.08 μmol/L, 0.02 μmol/L, and 0.03 μmol/L for Rhizon samplers, respectively. Both surface seawater and porewater samples were frozen at –20℃ until later analysis of nutrients. In addition, the sediment samples for the analysis of N content were placed in Ziploc plastic bags and then frozen at –20℃.

2.2 *Flow-through reactor experiments*

The flow-through reactor (FTR) experiment was implemented according to Ning et al. (2020) using Plexiglas columns (with an inner diameter of 4 cm) and lids designed by Rao et al. (2007), in which radial grooves were milled around the inflow and outflow ports. Briefly, homogenized sediment was packed into each Plexiglas column, and seawater was pumped from the bottom up through the sediments from a large carboy with continuous air flushing. During incubations, the sediment columns were immersed in a tank filled with seawater (an external temperature controller was used to control the ambient temperature). Flux measurements began 6 h after the start of the column percolation to acclimatize under the laboratory conditions. The measurements were conducted twice, with the intervals of 1 h, and the duration of measurements was within 2 h. At each sampling time, seawater samples for nutrient analysis were collected directly from the outflow, and the inflow seawater samples were collected from the source using 60 mL syringes. Additionally, an aliquot of seawater for N_2 measurement was sampled and transferred to a 12 mL Exetainer vial (Labco Ltd.), and the dissolved oxygen (DO) of inflow and outflow seawater was measured using a multiparameter probe (YSI ProDSS). The FTR experiments were carried out in duplicate.

Five experiments were performed covering the conditions summarized in Table 1. In the first experiment, sediments and seawater collected from each station were incubated to investigate the sedimentary N dynamics. In the second experiment, all the sediments collected from different stations were mixed and

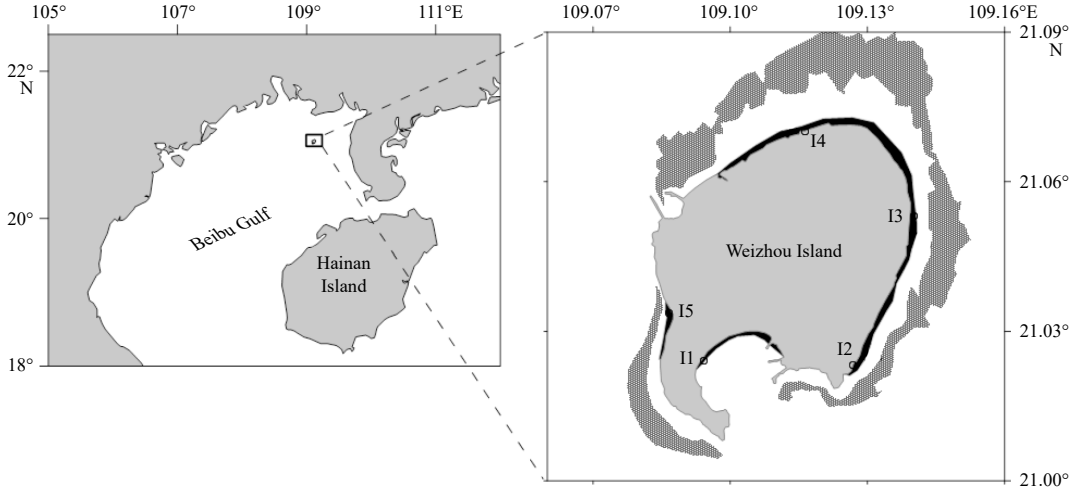

Fig. 1. Sampling stations in the tidal flats (the black areas) around Weizhou Island. The dark grey areas are coral covering areas. I1–I5 are the station IDs.

Table 1. Summary of conditions in flow-through reactor experiment

Experiment	Temperature/℃	NO_3^-/(μmol·L^{-1})	TOC content	Advection rate/(mL·min^{-1})	Column length/cm
1– Station	26	**see Table 2**	0.03%±0.01%	1	10
2– NO_3^- concentration	26	**1, 4, 10, 30, 45**	0.05%	1	10
3– TOC concentration	26	25±5	**0.05%, 0.14%, 0.22%**	1	10
4– Advection rate and flow path length	26	45±5	0.05%	**0.5, 1, 2, 3**	**5, 10, 15, 20**
5– Temperature	**20, 26, 32**	10±5	0.05%	1	10

Note: The variable parameters are indicated in bold.

Table 2. Nutrient concentrations in overlying seawater and porewater in sediments, and total nitrogen (TN) content in bulk sediments

Station	Seawater				Porewater				Sediment
	NH_4^+/ (μmol·L^{-1})	NO_2^-/ (μmol·L^{-1})	NO_3^-/ (μmol·L^{-1})	DIP/ (μmol·L^{-1})	NH_4^+/ (μmol·L^{-1})	NO_2^-/ (μmol·L^{-1})	NO_3^-/ (μmol·L^{-1})	DIP/ (μmol·L^{-1})	TN (dry weight)/ (μmol·g^{-1})
I1	0.70	0.33	4.36	0.02	6.72	3.16	6.76	0.46	2.90
I2	0.81	0.33	9.95	0.08	8.64	2.54	214.03	0.54	3.34
I3	1.14	0.30	1.44	0.08	113.28	0.81	0.43	0.54	4.28
I4	1.27	0.32	5.04	0.15	14.75	3.94	48.80	0.50	1.25
I5	2.02	0.46	9.28	0.43	156.03	1.29	0.56	0.69	2.47

repacked in FTRs, and different NO_3^- doses were added into the inflow seawater with the final NO_3^- concentrations of 1 μmol/L, 4 μmol/L, 10 μmol/L, 30 μmol/L, and 45 μmol/L, respectively. In the third experiment, sediments were mixed with different proportions of freeze-dried phytoplankton to obtain gradient TOC content of 0.05%, 0.14%, and 0.22%, and other variables were kept constant. The porewater flow rate in the former three experiments was maintained at 1 mL/min (equivalent to 48 L/(m^2·h)), with a residence time of 1 h. In the fourth experiment, mixed sediments were used as in the second experiment, and the seawater was pumped through the FTRs at variable flow rates (0.5 mL/min, 1 mL/min, 2 mL/min, and 3 mL/min); meanwhile, four column lengths (5 cm, 10 cm, 15 cm, and 20 cm) were used to assess how flow path lengths influence nutrient fluxes. In the fifth experiment, sediments were incubated at a temperature of 20℃, 26℃, and 32℃, respectively.

2.3 *Analytical methods*

Each frozen sediment sample was freeze-dried, and the total N (TN) content in sediment was determined using a CHNOS Elemental Analyzer (Vario EL III, Elemental Analyzer). The precision for TN had a <6% coefficient of variation (CV). Nutrient concentrations in seawater were determined using an autoanalyzer (QuAAtro, SEAL Analytical). The measurement precisions for the NO_3^-, NO_2^-, NH_4^+, dissolved inorganic phosphorus (DIP), and total dissolved nitrogen (TDN) analyses had a <6% CV. The dissolved organic nitrogen (DON) concentration was obtained from the difference between the TDN concentration and the dissolved inorganic nitrogen (DIN includes NO_3^-, NO_2^- and NH_4^+) concentration. The dissolved N_2 was measured by membrane inlet mass spectrometry.

2.4 *Calculations and statistical analyses*

Fluxes (F, mmol/(m^2·h)) were calculated from the differences in the concentrations of NO_3^-, NO_2^-, NH_4^+, DIP, DO, and N_2 between the influent and effluent seawater, flow rate, and cross-sectional area of the sediment column according to Eq. (1). Positive values represent an efflux out of the sediment, whereas negative values represent an influx into the sediment.

$$F = (C_{out} - C_{in}) \times R/S, \quad (1)$$

where, C_{in} and C_{out} are the concentrations of NO_3^-, NO_2^-, NH_4^+, DIP, DO, and N_2 in the influent and effluent seawater, respectively. R is the flow rate, and S is the cross-sectional area of the sediment column (12.56 cm^2).

Pearson's correlation analysis with a two-tailed test of significance was used to evaluate the relationship between the parameters. Statistical analyses were carried out using the Statistical Package for the Social Sciences (SPSS) software (version 22.0), and the statistical significance was judged at the criterion of p< 0.05.

3 Results

3.1 *N and P contents in the surface seawater and sediment around the Weizhou Island during September 2019*

The average concentrations of NH_4^+, NO_2^-, and NO_3^- in the surface seawater of Weizhou Island were (1.19±0.52) μmol/L, (0.35±0.06) μmol/L, and (6.01±3.56) μmol/L, respectively (Table 2). NO_3^- dominated the DIN, and the concentration of DIN was 27–399 times that of DIP ((0.15±0.16) μmol/L). The nutrient concentrations in porewater were several times or even dozens of times higher than those in surface seawater, but the concentrations were significantly different among different stations (Table 2). The proportion of NH_4^+ in DIN in porewater was significantly higher than that in surface seawater, especially at Stations I3 and I5, in which NH_4^+ absolutely dominated the DIN. The DIP concentration in porewater ranged from 0.46 μmol/L to 0.69 μmol/L, and the ratio of DIN:DIP was 24–418. The TN content in the sediments of Weizhou Island was as low as 1.25–4.28 μmol/g.

3.2 *The first FTR experiment: clear release of N_2 of sediment of all sites*

The NH_4^+ was released from the sediment into the seawater at rate of 0.01–0.04 mmol/(m^2·h), but was transferred from the seawater into the sediment at Station I5; NO_2^- and NO_3^- were transferred from the seawater into the sediments at the rate of 0.01–0.02 mmol/(m^2·h) and 0.01–0.25 mmol/(m^2·h), respectively (Fig. 2). Meanwhile, the N_2 flux (0.11–0.25 mmol/(m^2·h)) is equivalent to or even greater than the DIN efflux (Fig. 2).

There were significant differences in the N flux among stations at Weizhou Island, not only in the order of magnitude but also in the flux direction (Fig. 2). For example, the N flux at Station I5 was differed significantly from that at other stations, and the influx of NH_4^+ and the efflux of NO_3^- were observed at this sta-

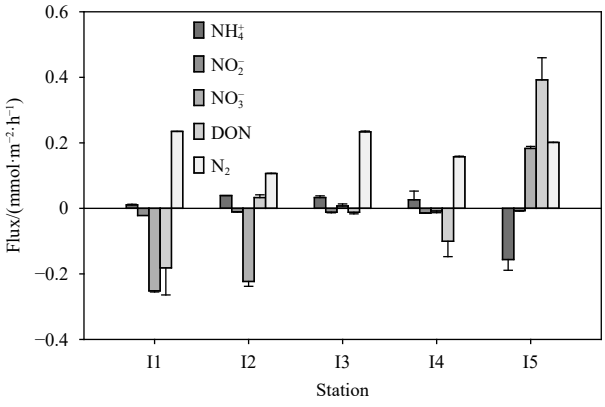

Fig. 2. Fluxes of different N forms at the seawater-sediment interface of different stations at Weizhou Island during September 2019.

Table 3. Correlation analysis results for NO_3^- and DIP concentrations in seawater and the TN in sediments and fluxes of DO, N_2, DIN, and DON obtained from the first FTR experiment

	NO_3^- concentration	DIP concentration	TN concentration	DO flux	N_2 flux	DIN flux
DIP concentration	0.23					
TN concentration	0.22	−0.02				
DO flux	−0.05	0.13	−0.45*			
N_2 flux	−0.72*	0.01	0.05	−0.04		
DIN flux	−0.65*	0.34	−0.06	0.18	0.47*	
DON flux	0.34	0.92*	0.00	0.17	−0.20	0.34

Note: * correlation is significant at the 0.05 level, n=20.

tion, reflecting the strong nitrification occurring in the sediments of this station. The N_2 flux was positively correlated with the DIN flux, but the N_2 flux was negatively correlated with the NO_3^- concentration in the seawater (Table 3). Although complicated, DON flux (−0.18–0.39 mmol/(m²·h)) was related to the dissolution and adsorption of particulate organic N, exhibiting significant spatial differences in magnitude and direction.

3.3 *The second FTR experiment: the increasing NO_3^- concentration corresponded to the increasing NO_3^- influx into the sediment*

The second FTR experiment with different NO_3^- concentrations of 1 μmol/L, 4 μmol/L, 10 μmol/L, 30 μmol/L, and 45 μmol/L was implemented to access the effect of the increasing NO_3^- on the N flux at the seawater–sediment interface of Weizhou Island. When the concentration of NO_3^- in seawater was lower than (2.4±4.3) μmol/L, NO_3^- was released from the sediment to the seawater at a rate of >0.19 mmol/(m²·h), but when the concentration was higher than this threshold, NO_3^- was transferred from the seawater to the sediment, and the influx of NO_3^- increased with the increasing concentration of NO_3^- (Fig. 3).

3.4 *The third FTR experiment: the increasing TOC corresponded to the increase of NH_4^+ and DON output, and NO_3^- input from the sediment to the seawater*

The release rates of NH_4^+ and DON from the sediment to the seawater gradually increased with the increase of TOC content, and the consumption rate of NO_3^- in sediment also increased at the same time (Fig. 4). However, the NH_4^+ flux (<0.008 mmol/(m²·h)) was negligible in comparison with NO_3^- flux (−0.88 mmol/(m²·h) to −0.70 mmol/(m²·h)) and DON flux (0.02–1.04 mmol/(m²·h)).

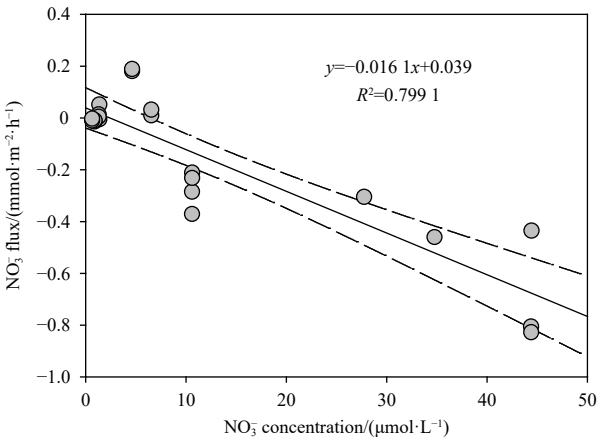

Fig. 3. Relationship between NO_3^- flux and NO_3^- concentration in the influent seawater of flow-through reactor. Dashed lines represent 95% confidence intervals.

3.5 *The fourth FTR experiment: a selective increase of NO_3^- and DON fluxes at the intermediate advection rate and flow length*

The peak of NO_3^- influx was observed at the intermediate advection rate (96 L/(m²·h)), and NO_3^- also peaked at the intermediate flow path length (10 cm) under intermediate advection (Fig. 5a). Meanwhile, because the TOC contents in sediments were low, the NH_4^+ released by mineralization was insignificant under variable advection rates and flow path lengths (Fig. 5b). Similar to NO_3^- flux, DON efflux peaked at the intermediate advection rate (96 L/(m²·h)) and flow path length (10 cm; Fig. 5c).

3.6 *The fifth FTR experiment: temperature significantly affected sedimentary N dynamics at Weizhou Island*

The flux of various forms of N increased with the increase of

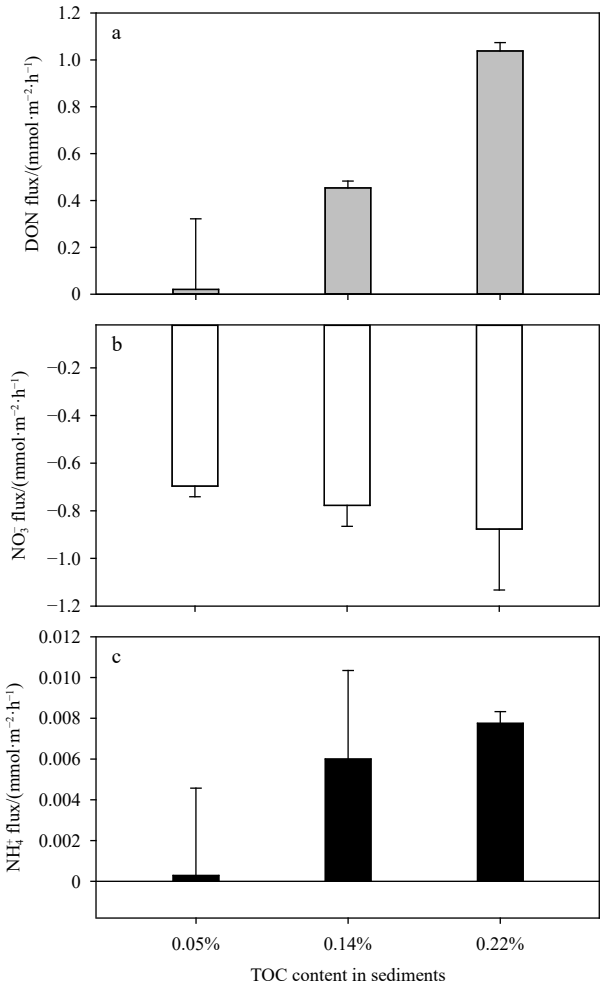

Fig. 4. Fluxes of DON (a), NO_3^- (b), and NH_4^+(c) under variable TOC contents.

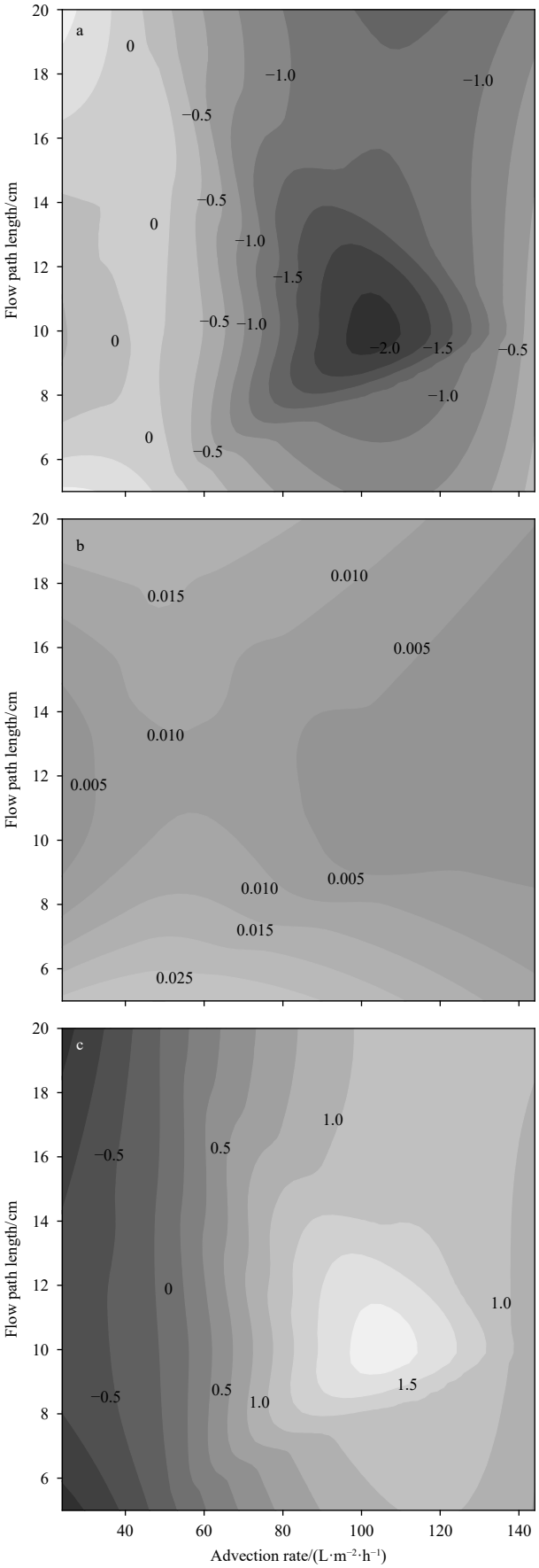

Fig. 5. Fluxes (isoline, mmol/(m²·h)) of NO_3^- (a), NH_4^+ (b), and DON (c) under different advection conditions.

temperature from 20℃ to 32℃ (Fig. 6), indicating that the increase of temperature promoted the activity of the bacteria involved in N cycling in sediments. However, the DON flux decreased significantly to (0.13±0.14) mmol/(m²·h) at 26℃ (Fig. 6a), indicating that there was a process consuming DON, such as the degradation of DON to NH_4^+. Indeed, the highest NH_4^+ efflux was observed at the same temperature ((0.07±0.02) mmol/(m²·h); Fig. 6b). When the temperature rose to 32℃, only DON released by the dissolution of refractory organic matter was stimulated, probably due to the low proportion of degradable organic matter in total organic matter content. Therefore, the DON flux significantly increased to (1.23±0.02) mmol/(m²·h), but the NH_4^+ flux did not increase significantly (Fig. 6).

At the temperature of 20℃, NO_3^- was released from sediment to seawater at a flux of (0.05±0.22) mmol/(m²·h), but when the temperature increased to 26℃, NO_3^- was transferred from seawater to sediment ((0.25±0.12) mmol/(m²·h)), and the magnitude of its influx increased with the increase of temperature (Fig. 6c).

4 Discussion

4.1 *High potential rates of sedimentary N transformation at Weizhou Island during September 2019*

Clear release of N_2 from sediments was observed at all sites (Fig. 2), and the sedimentary N removal pathway would deplete

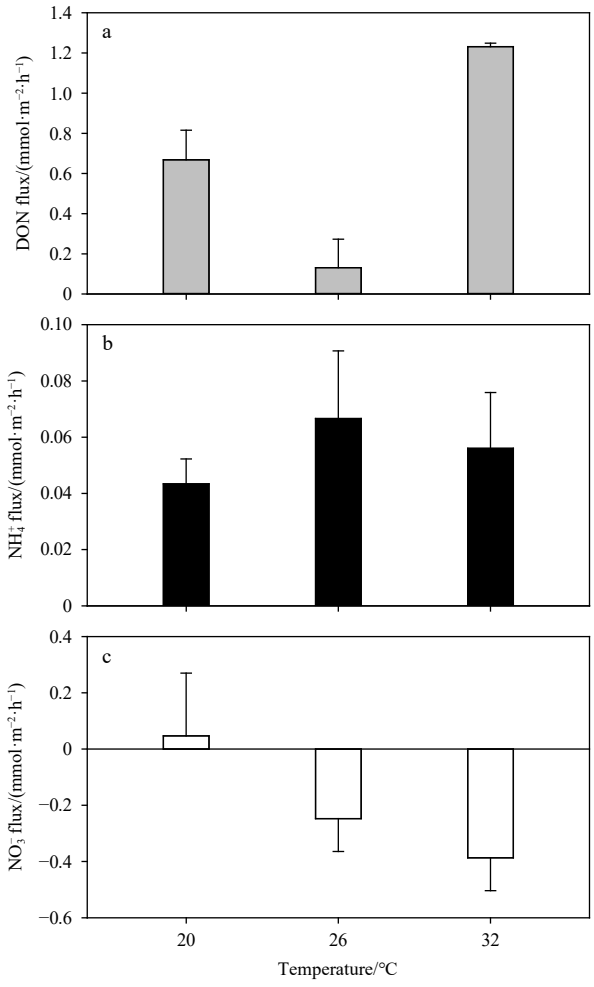

Fig. 6. Fluxes of DON (a), NH_4^+ (b), and NO_3^- (c) under variable temperature conditions.

the NO_3^- in water column within a couple of days. Indeed, it seems the sedimentary N flux measured here were quite high in comparison with those in other coral reefs measured by benthic chamber or intact core incubation (Eyre et al., 2008). Previous studies have assessed the limitation of FTRs, because fixed porewater advection rate, flow paths or compositions of inflow seawater are far from the natural conditions (Santos et al., 2012; Ning et al., 2019). Thus, these fluxes measured by FTRs may represent potential rates for the Weizhou Island sediments. Furthermore, benthic categories of coral reefs include corals, turf algae, biogenic rock, etc., besides sediments, and N_2 flux varied significantly at different categories (El-Khaled et al., 2021). Thus, we should avoid direct extrapolations from the laboratory results to field conditions.

The potential rate of NH_4^+ relese from the Weizhou Island sediments (0.01–0.04 mmol/(m²·h), Fig. 2) was much lower than that of the Great Barrier Reef (about 0.5 mmol/(m²·h); Santos et al., 2012). One explanation is because the TN content in the sediments of Weizhou Island (1.25–4.28 μmol/g) was lower than that in the sediments of the Great Barrier Reef (19–44 μmol/g; Alongi et al., 2008). Indeed, DO flux (an indicator of mineralization rate) was closely related to the TN content in the sediments (Table 3). An alternative explanation is that most of the NH_4^+ released by mineralization of organic matter was adsorbed within porous carbonate sand grains or was consumed by nitrifying bacteria (Jäntti et al., 2011).

The N_2 flux here are supposed to be the potential rate of denitrification, because the N_2 fixation (N_2 consumption) and anammox (N_2 production) in the Weizhou Island sediments was negligible (Ning et al., 2022). In general, coupled nitrification-denitrification is active in permeable sand sediments (Marchant et al., 2016), which explains why N_2 flux was positively correlated with DIN flux (Table 3). The sufficient DO in the surface permeable sediments enhances the rates of nitrification and its coupled denitrification (Rysgaard et al., 1994). In similar, the N_2 flux was negatively correlated with the NO_3^- concentration in the seawater (Table 3), indicating that denitrification in the sediment of Weizhou Island depended on the NO_3^- provided by nitrification rather than the NO_3^- in the overlying seawater. However, the availability of organic matter and its degradation product (i.e., NH_4^+) is a limiting factor of nitrification (Jäntti et al., 2011; Rysgaard et al., 1994), which explains why NH_4^+ was transferred from the seawater into the sediment at Station I5 (Fig. 2).

4.2 *Inorganic N retaining within the sediments versus losing as N_2 products*

FTR experiments allow the manipulation of experimental conditions to gain insights into the mechanisms controlling the N dynamics in permeable sediments (Santos et al., 2012). Through changing flow rates and flow length, a peak of NO_3^- influx was also observed at the intermediate advection rate (96 L/(m²·h); Fig. 5a) because the intermediate advection rate enhances the development of the microenvironment (i.e., steep DO gradients) within porous carbonate sediments, perhaps providing optimal conditions for the dissimilatory reduction of the external NO_3^- transmitted to the microenvironment (Santos et al., 2012). Furthermore, NO_3^- influx also peaked at the intermediate flow path length (10 cm) under intermediate advection (Fig. 5a), indicating that there may be an oxidation process in the deeper layer of sediment (>10 cm), which results in the reproduction of NO_3^- (Zhang and Furman, 2021). If NO_3^- was reduced to N_2 by denitrifiers, NO_3^- reproduction would not occur; thus, the possible explanation is that NO_3^- was mainly reduced to NH_4^+ by dissimilatory nitrate reduction to ammonium (DNRA) bacteria, and when these NH_4^+ accumulated to a certain concentration within the anoxic microenvironment, they were transferred to the external oxic environment where they were reoxidized to NO_3^-. However, the NH_4^+ flux was insignificant in comparison with those of other N forms (Fig. 5b), perhaps because of the adsorption of NH_4^+ by sediment pores (Mackin and Aller, 1984).

In short, a selective increase of NO_3^- flux at given advection rate and flow length showed that more inorganic N was retained within the sediments than lost as N_2 products. Meanwhile, DON can be released during growth of denitrification or DNRA bacteria (Kawasaki and Benner, 2006), resulting in greatest DON efflux at this situation (Fig. 5c). Thus, the interaction between currents and seabed topography makes permeable carbonate sands acting as reservoir of N. This implies that permeable carbonate sands may help to buffer coral reefs during periods of eutrophication or extreme oligotrophy (Erler et al., 2014).

4.3 *Implication for the N dynamics in reef sediments under the influences of climate warming and anthropogenic activities*

The increasing anthropogenic pollution has resulted in an increasing trend in NO_3^- concentration (Yu et al., 2019; Pan et al., 2021). Thus, N-excess conditions occurred at Weizhou Island, which was consistent with other reefs affected by anthropogenic activities (Lapointe et al., 2019; Guo et al., 2019). The input of anthropogenic NO_3^- may be transferred into the sediment, and the influx of NO_3^- increased with the increasing NO_3^- concentration in seawater (Fig. 3). This is consistent with the finding in a intertidal flat (Jiang et al., 2021), indicating that water NO_3^- directly regulated the N flux between seawater and permeable sediments (Wang et al., 2021). However, denitrification did not benefit from the increase of NO_3^-, indicated by the negative relationship between N_2 flux and NO_3^- concentration in seawater (Table 3). Thus, the anthropogenic NO_3^- would be retained in the sediment as adsorbed NH_4^+ following DNRA.

Anthropogenic sediment loads could impact on coral bleaching (Baird et al., 2021) and lead to the increase of DON released from the sediment (Fig. 4a), which enhances the risk of eutrophication in N-excess areas (Lu et al., 2020) such as Weizhou Island. Meanwhile, the increase of TOC content promoted the consumption of NO_3^- in sediments (Fig. 4b), because the availability of organic matter limits the potential denitrification rate of heterotrophic denitrifiers (Deek et al., 2012).

Temperature is a key factor affecting benthic N flux (Tan et al., 2020; Canion et al., 2014; Muta et al., 2020). The optimal activity temperature of denitrifying bacteria is greater than 25℃ (Tan et al., 2020), which can explain the increase of NO_3^- consumption in sediments due to temperature rise. However, DNRA bacteria are also thermophilic (Rahman et al., 2019). With the impacts of anthropogenic activities and global warming, further studies using isotope tracing technology and gene sequencing are still needed to assess whether the dissimilatory reduction of NO_3^- in carbonate sands is mainly regeneration by DNRA or removal by denitrification. However, the increase of DON flux was much greater than that of NO_3^- flux, and thus, the impacts of anthropogenic activities and climate warming will exacerbate the N-excess condition in Weizhou Island reefs.

5 Conclusions

We conducted a series of FTR experiments to investigate the mechanisms controlling the N dynamics in permeable carbon-

ate sands. The results indicated that permeable carbonate sands act as reservoirs of N under the influence of advective flow, but the sedimentary N dynamics had limited contributions to the N removal at Weizhou Island reefs under N-excess conditions. In the future, the escalating anthropogenic activities (enrichments of NO_3^- in seawater and TOC in sediments) and climate change (increasing temperatures) will exacerbate the N-excess condition in Weizhou Island reefs. However, further studies on N dynamics in benthic categories of coral reefs include corals, turf algae, sediments, biogenic rock using isotope tracing technology are still needed to reveal the N cycling in coral reefs.

References

Alongi D M, Trott L A, Pfitzner J. 2008. Biogeochemistry of inter-reef sediments on the northern and central Great Barrier Reef. Coral Reefs, 27(2): 407–420, doi: 10.1007/s00338-007-0347-2

Baird M E, Mongin M, Rizwi F, et al. 2021. The effect of natural and anthropogenic nutrient and sediment loads on coral oxidative stress on runoff-exposed reefs. Marine Pollution Bulletin, 168: 112409, doi: 10.1016/j.marpolbul.2021.112409

Canion A, Kostka J E, Gihring T M, et al. 2014. Temperature response of denitrification and anammox reveals the adaptation of microbial communities to *in situ* temperatures in permeable marine sediments that span 50° in latitude. Biogeosciences, 11(2): 309–320, doi: 10.5194/bg-11-309-2014

Cook P L M, Kessler A J, Eyre B D. 2017. Does denitrification occur within porous carbonate sand grains?. Biogeosciences, 14(18): 4061–4069

Deek A, Emeis K, van Beusekom J. 2012. Nitrogen removal in coastal sediments of the German Wadden Sea. Biogeochemistry, 108(1–3): 467–483

Eakin C M, Sweatman H P A, Brainard R E. 2019. The 2014–2017 global-scale coral bleaching event: insights and impacts. Coral Reefs, 38(4): 539–545, doi: 10.1007/s00338-019-01844-2

El-Khaled Y C, Roth F, Rädecker N, et al. 2021. Nitrogen fixation and denitrification activity differ between coral- and algae-dominated Red Sea reefs. Scientific Reports, 11(1): 11820, doi: 10.1038/s41598-021-90204-8

Erler D V, Santos I R, Eyre B D. 2014. Inorganic nitrogen transformations within permeable carbonate sands. Continental Shelf Research, 77: 69–80, doi: 10.1016/j.csr.2014.02.002

Eyre B D, Glud R N, Patten N. 2008. Mass coral spawning: a natural large-scale nutrient addition experiment. Limnology and Oceanography, 53(3): 997–1013, doi: 10.4319/lo.2008.53.3.0997

Guo Jing, Yu Kefu, Wang Yinghui, et al. 2019. Potential impacts of anthropogenic nutrient enrichment on coral reefs in the South China Sea: evidence from nutrient and chlorophyll *a* levels in seawater. Environmental Science: Processes & Impacts, 21(10): 1745–1753

Hughes T P, Baird A H, Bellwood D R, et al. 2003. Climate change, human impacts, and the resilience of coral reefs. Science, 301(5635): 929–933, doi: 10.1126/science.1085046

Hughes T P, Kerry J T, Álvarez-Noriega M, et al. 2017. Global warming and recurrent mass bleaching of corals. Nature, 543(7645): 373–377, doi: 10.1038/nature21707

Jäntti H, Stange F, Leskinen E, et al. 2011. Seasonal variation in nitrification and nitrate-reduction pathways in coastal sediments in the Gulf of Finland, Baltic Sea. Aquatic Microbial Ecology, 63(2): 171–181, doi: 10.3354/ame01492

Jiang Shan, Kavanagh M, Ibánhez J S P, et al. 2021. Denitrification-nitrification process in permeable coastal sediments: an investigation on the effect of salinity and nitrate availability using flow-through reactors. Acta Oceanologica Sinica, 40(9): 1–12, doi: 10.1007/s13131-021-1811-5

Kawasaki N, Benner R. 2006. Bacterial release of dissolved organic matter during cell growth and decline: molecular origin and composition. Limnology and Oceanography, 51(5): 2170–2180, doi: 10.4319/lo.2006.51.5.2170

Kessler A J, Cardenas M B, Santos I R, et al. 2014. Enhancement of denitrification in permeable carbonate sediment due to intragranular porosity: a multi-scale modelling analysis. Geochimica et Cosmochimica Acta, 141: 440–453, doi: 10.1016/j.gca.2014.06.028

Lapointe B E, Brewton R A, Herren L W, et al. 2019. Nitrogen enrichment, altered stoichiometry, and coral reef decline at Looe Key, Florida Keys, USA: a 3-decade study. Marine Biology, 166(8): 108, doi: 10.1007/s00227-019-3538-9

Lu Dongliang, Kang Zhenjun, Yang Bin, et al. 2020. Compositions and spatio-temporal distributions of different nitrogen species and lability of dissolved organic nitrogen from the Dafengjiang River to the Sanniang Bay, China. Marine Pollution Bulletin, 156: 111205, doi: 10.1016/j.marpolbul.2020.111205

Mackin J E, Aller R C. 1984. Ammonium adsorption in marine sediments. Limnology and Oceanography, 29(2): 250–257, doi: 10.4319/lo.1984.29.2.0250

Marchant H K, Holtappels M, Lavik G, et al. 2016. Coupled nitrification-denitrification leads to extensive N loss in subtidal permeable sediments. Limnology and Oceanography, 61(3): 1033–1048, doi: 10.1002/lno.10271

Morris L A, Voolstra C R, Quigley K M, et al. 2019. Nutrient availability and metabolism affect the stability of coral–symbiodiniaceae symbioses. Trends in Microbiology, 27(8): 678–689, doi: 10.1016/j.tim.2019.03.004

Muta N, Umezawa Y, Yamaguchi A, et al. 2020. Estimation of spatiotemporal variations in nutrient fluxes from sediments in the seasonally hypoxic Omura Bay, Japan. Limnology, 21(3): 341–356, doi: 10.1007/s10201-019-00591-1

Ning Zhiming, Fang Cao, Yu Kefu, et al. 2020. Influences of phosphorus concentration and porewater advection on phosphorus dynamics in carbonate sands around the Weizhou Island, northern South China Sea. Marine Pollution Bulletin, 160: 111668, doi: 10.1016/j.marpolbul.2020.111668

Ning Zhiming, Yu Kefu, Wang Yinghui, et al. 2019. Carbon and nutrient dynamics of permeable carbonate and silicate sands adjacent to coral reefs around Weizhou Island in the northern South China Sea. Estuarine, Coastal and Shelf Science, 225: 106229

Ning Zhiming, Yu Kefu, Wang Yinghui, et al. 2022. Effects of nutrient enrichment and skewed N: P ratios on physiology of scleractinian corals from Weizhou Island in the northern South China Sea. Marine Ecology Progress Series, 682: 111–122, doi: 10.3354/meps13933

Pan Ke, Zheng Xinqing, Liu Xinming, et al. 2021. Nitrogen cycling in a tropical coral reef ecosystem under severe anthropogenic disturbance in summer: insights from isotopic compositions. Water Research, 207: 117824, doi: 10.1016/j.watres.2021.117824

Rahman M, Grace M R, Roberts K L, et al. 2019. Effect of temperature and drying-rewetting of sediments on the partitioning between denitrification and DNRA in constructed urban stormwater wetlands. Ecological Engineering, 140: 105586, doi: 10.1016/j.ecoleng.2019.105586

Rao A M F, McCarthy M J, Gardner W S, et al. 2007. Respiration and denitrification in permeable continental shelf deposits on the South Atlantic Bight: Rates of carbon and nitrogen cycling from sediment column experiments. Continental Shelf Research, 27: 1801–1819, doi: 10.1016/j.csr.2007.03.001

Rasheed M, Badran M I, Huettel M. 2003. Particulate matter filtration and seasonal nutrient dynamics in permeable carbonate and silicate sands of the Gulf of Aqaba, Red Sea. Coral Reefs, 22(2): 167–177, doi: 10.1007/s00338-003-0300-y

Robertson E K, Bartoli M, Brüchert V, et al. 2019. Application of the isotope pairing technique in sediments: use, challenges, and new directions. Limnology and Oceanography: Methods, 17(2): 112–136, doi: 10.1002/lom3.10303

Rosset S, Wiedenmann J, Reed A J, et al. 2017. Phosphate deficiency promotes coral bleaching and is reflected by the ultrastructure of symbiotic dinoflagellates. Marine Pollution Bulletin, 118(1–2): 180–187

Rysgaard S, Risgaard-Petersen N, Niels Peter S, et al. 1994. Oxygen regulation of nitrification and denitrification in sediments. Lim-

nology and Oceanography, 39(7): 1643–1652, doi: 10.4319/lo.1994.39.7.1643

Santos I R, Eyre B D, Glud R N. 2012. Influence of porewater advection on denitrification in carbonate sands: evidence from repacked sediment column experiments. Geochimica et Cosmochimica Acta, 96: 247–258, doi: 10.1016/j.gca.2012.08.018

Tan Ehui, Zou Wenbin, Zheng Zhenzhen, et al. 2020. Warming stimulates sediment denitrification at the expense of anaerobic ammonium oxidation. Nature Climate Change, 10(4): 349–355, doi: 10.1038/s41558-020-0723-2

Wang Weilei, Moore J K, Martiny A C, et al. 2019. Convergent estimates of marine nitrogen fixation. Nature, 566(7743): 205–211, doi: 10.1038/s41586-019-0911-2

Wang Weibo, Wang Xu, Shu Xiao, et al. 2021. Denitrification of permeable sand sediment in a headwater river is mainly influenced by water chemistry, rather than sediment particle size and heterogeneity. Microorganisms, 9(11): 2202, doi: 10.3390/microorganisms9112202

Wiedenmann J, D'Angelo C, Smith E G, et al. 2013. Nutrient enrichment can increase the susceptibility of reef corals to bleaching. Nature Climate Change, 3(2): 160–164, doi: 10.1038/nclimate1661

Wild C, Rasheed M, Jantzen C, et al. 2005. Benthic metabolism and degradation of natural particulate organic matter in carbonate and silicate reef sands of the northern Red Sea. Marine Ecology Progress Series, 298: 69–78, doi: 10.3354/meps298069

Xie Lei, Gao Xuelu, Liu Yongliang, et al. 2021. Perpetual atmospheric dry deposition exacerbates the unbalance of dissolved inorganic nitrogen and phosphorus in coastal waters: a case study on a mariculture site in North China. Marine Pollution Bulletin, 172: 112866, doi: 10.1016/j.marpolbul.2021.112866

Yang S, Gruber N. 2016. The anthropogenic perturbation of the marine nitrogen cycle by atmospheric deposition: nitrogen cycle feedbacks and the ^{15}N Haber-Bosch effect. Global Biogeochemical Cycles, 30(10): 1418–1440, doi: 10.1002/2016GB005421

Yu Wanjun, Wang Wenhuan, Yu Kefu, et al. 2019. Rapid decline of a relatively high latitude coral assemblage at Weizhou Island, northern South China Sea. Biodiversity and Conservation, 28(14): 3925–3949, doi: 10.1007/s10531-019-01858-w

Zhang Zengyu, Furman A. 2021. Redox dynamics at a dynamic capillary fringe for nitrogen cycling in a sandy column. Journal of Hydrology, 603: 126899, doi: 10.1016/j.jhydrol.2021.126899